Research Article J. Electrochem. Sci. Technol., 2024, 15(3), 414-420

Empirical Capacity Degradation Model for a Lithium-Ion Battery Based on Various C-Rate Charging Conditions

Dong Hyun Kim[1,2,3], Juhyung Lee[4], Kyungseop Shin[5]*, Kwang-Bum Kim[2]*, and Kyung Yoon Chung[1]*

[1]*Energy Storage Research Center, Korea Institute of Science and Technology (KIST), 5, Hwarang-ro 14-gil, Seongbuk-gu, Seoul 02792, Republic of Korea*

[2]*Department of Materials Science and Engineering, Yonsei University, 134 Shinchon-dong, Seodaemoon-gu, Seoul 03722, Republic of Korea*

[3]*R&D center, Remplir Inc., 129 Songsansandan-gil, Songsan-myeon, Hwaseong-si, Gyeonggi-do, 18545, Republic of Korea*

[4]*Consumer Product Division & Leisure Product Center, Korea Conformity Laboratories(KCL), 199, Gasan digital 1-ro, Geumcheon-gu, Seoul, 08503, Republic of Korea*

[5]*Department of Computer Science, Sangmyung University, Hongjimun 2-gil 20, Jongno-gu, Seoul, 03016, Republic of Korea*

ABSTRACT

Lithium-ion batteries are widely used in many applications due to their high energy density, high efficiency, and excellent cycle ability. Once an unknown Li-ion battery is reusable, it is important to measure its lifetime and state of health. The most favorable measurement method is the cycle test, which is accurate but time- and capacity-consuming. In this study, instead of a cycle test, we present an empirical model based on the C-rate test to understand the state of health of the battery in a short time. As a result, we show that the partially accelerated charge/discharge condition of the Li-ion battery is highly effective for the degradation of battery capacity, even when half of the charge/discharge conditions are the same. This observation provides a measurable method for predicting battery reuse and future capacity degradation.

Keywords : Capacity degradation model, Lithium ion battery, C-rate, Charging condition, Emperical

Received : 19 February 2024, Accepted : 9 April 2024

1. Introduction

Lithium-ion batteries (LIBs) are rechargeable energy storage devices based on high energy density intercalation. They are used in a wide range of applications, from small electronic devices to electric vehicles. Since the usage of the batteries gets more extensive, making good performance and high reliability gets more critical. The battery loses capacity defined by the ampere time (Ah) during the charge and discharge cycles. This capacity reduction results from various battery failure mechanisms; porosity degradation of the electrode, the formation and growth of a solid electrolyte intermediate phase (SEI) layer, electrolyte decomposition, and cracking of electrode particles. These failure mechanisms also affect the impedance and coulomb efficiency of the batteries [1]. LIB reliability tests are mainly performed by monitoring the battery capacity degradation due to repeated charge/discharge cycles.

The prediction of the remaining lifetime of a battery management system relies mainly on mechanical and semi-empirical models for battery state estimations. Many previous studies have modeled the state of LIBs [2], providing semi-experiential models to predict capacity loss. They have proposed semi-empirical and physical models that describe various mechanisms, including solid-electrolyte intermediate phase growth, active material loss, lithium plating, and increasing impedance. Diagnostic measurements such as impedance spectroscopy and coulombic efficiency can also be utilized for lifetime estimation. While this chemical and physical mechanism-based model demonstrates good prediction, statistical and

*E-mail address: ksshin@smu.ac.kr (K. Shin), kbkim@yonsei.ac.kr (K.-B. Kim), kychung@kist.re.kr (K. Y. Chung)

DOI: https://doi.org/10.33961/jecst.2024.00241

machine learning approaches to predict cell lifetime are attractive and good diagnostic alternatives [3]. Recent advances in computing power and data generation techniques have accelerated progress in various tasks, including predicting battery health properties, identifying chemical synthesis paths, and discovering materials for energy storage and catalysis.

Much effort has been made to develop new methods for estimating the status of health (SOH) of LIBs [4]. The Kalman filter has been proposed to estimate the state of charge (SOC) and SOH of LIBs. Particle filters are presented to estimate the internal resistance and SOH of LIBs based on the SOC and operational temperature [5]. These stochastic filtering methods are based on degradation models, and estimation performance is affected by the modeling complexity.

Recently, many researchers have actively studied machine learning techniques to estimate the SOH of LIBs by monitoring correlated data, such as voltage, current, temperature, and charge rate. A support vector machine algorithm estimated capacity fading from seven cells under the 1% error range with partial charge data. This method using available online data has demonstrated good accuracy for SOH estimation under electric vehicles' operating conditions. To ensure high precision of the SOH estimation, back-propagation-based neural networks have been adopted [6]. This research verified the equivalent circuit model parameters of the battery using the direct parameter extraction derived by the hybrid pulse power test. To illustrate the tendency of the degradation learning time under various charging rates and operating temperature conditions, a short- and long-term memory-based approach was also proposed.

A continuous cycle test is one of the most general types of battery cycle tests in which batteries are continuously charged and discharged between the manufacturer-specified discharge and charge end voltages [7]. This test calculates the battery discharge capacity in each cycle, which results in a trend of capacity reduction. Therefore, a stress variable in the continuous cycle test of a LIB was considered. The normalized battery discharge current is typically depicted as the C-rate. For example, a 1.5 A current for a 1500 mAh battery represents 1 C of the C-rate.

Acceleration tests are performed by raising the product's load conditions to assess its reliability quickly [8]. For LIBs, an accelerated discharge C-rate is one of the acceleration tests. The capacity reduction was recorded during the test in different cycles. This acts as an indicator of battery degradation. In this type of acceleration test, the deterioration indicators of the batteries were continuously recorded during the test or at a certain point to capture the deterioration process. The battery capacity degradation measurements can be used to model the degradation process.

2. Capacity degradation model

Many failure mechanisms cause the capacity degradation of LIBs. The side reaction between the anode and electrolyte eliminates active lithium and forms an SEI layer on the anode. The SEI layer is usually the primary failure mechanism for LIBs in storage and cycling operations. In particular, the effect of discharge rates at the combination of four different C-rates, namely 0.2, 0.5, 1, and 2 C, on the capacity degradation of LIBs was studied, and it was concluded that a higher C-rate accelerates the growth of the SEI layer. The temperature increase by ohmic heating could encounter pressure accumulation because of the electrolytes' evaporation and the generation of gas products, resulting in cracks on the film surface. Such damages cause side reactions between the electrolyte and the lithiated carbon, making the SEI layer thicker.

Carnovale *et al.* developed a mathematical model that calculates the profile of concentration, expansion, and contraction during the extraction and intercalation of lithium into spherical particles of electrode materials [9]. Their simulations showed that high-power applications have a higher chance of particle destruction compared to low-power applications. These damages may result in the SEI layer growth. Recently, many works have found the semi-empirical model to be a suitable mathematical model representing experimental results rather than a physical model [10–12]. As they investigated, the empirical battery data is not fully understood via the physical model because they are mainly affected by the dominant charge/discharge conditions. This paper suggests that the SEI layer continues to be a remarkable failure mechanism of the LIB during accelerated operation condition-based cycling.

If the discharge C-rate increases, the speed of SEI layer growth would be further accelerated with the electrode particles and surface film cracking by over-

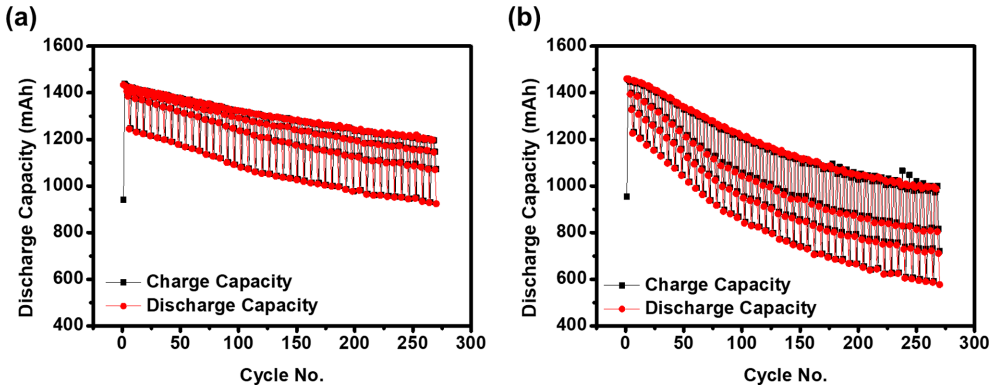

Fig. 1. Discharge capacity vs. cycle test results with different charge conditions, namely (a) 0.5 C for Case 1 and (b) 1.0 C for Case 2.

heating. The destruction coefficient is a function of operating temperature, which relies on the environmental temperature and C-rate causing ohmic heating. The increased battery current makes it more susceptible to electrode particles and cracks in the SEI layer [13]. Since such a crack may provide a new part for reducing the electrolyte, the C-rate may affect the effective anode region to which the electrolyte may be accessed. Therefore, the effects of C-rate and temperature on degradation level in the n^{th} cycle, D(n), are formalized by the generalized power law model [8] as follows:

$$D(n) = a \cdot n^{\alpha} + b\,, \tag{1}$$

where a is the degradation coefficient, which is the function of C-rate and temperature derived at Eq. (2), α is the power-law coefficient, and b is the offset. The generalized Eyring model format is adopted to analyze the effect of temperature, thermal stress, discharge C-rate, and non-thermal stress on D(n) [14]. The generalized Eyring model is generally used to model relationships between thermal and non-thermal stress under chemical reaction-based mechanisms. These interactions significantly affect the battery capacity degradation performance. The coefficient $a = E(V, U)$ is a function of the thermal stress V and specific stress U, given as follows:

$$a = A_V \exp\left\{\frac{B}{V} + \left(C + \frac{D}{V}\right)U\right\}, \tag{2}$$

where A_V, B, C, and D are the coefficients of the generalized Eyring model. The non-thermal stress U consists of the charge and discharge current and voltage. As the thermal and non-thermal stresses increase, the capacity degradation increases accordingly.

Variations in the C-rate were employed in this study. Previous studies have assumed that the charge and discharge C-rates are constant during the cycle testing period. However, in practice, a battery is not constantly charged or discharged. We have investigated mathematical pattern-matching models such as polynomials, power series, rational function, exponential, Gaussian models to reflect the degradation performance of various C-rate in that the polynomial model showed the lowest fitting error. To describe the effect of the variable charging conditions, we modified the diffusivity model (2) by converting a constant b to a function of the number of cycles $b(n)$, as follows:

$$b(n) = a' n^{\beta} + b_0\,, \tag{3}$$

where a' is a degradation coefficient derived from the inevitable change in charging conditions, β is an exponent caused by variable charging conditions, and b_0 is an offset to fit this model to the data.

3. Experimental

Commercial 18650 cells were provided by Remplir Inc. (Chuncheon, Republic of Korea). The cell exhibited a capacity of approximately 1500 mAh and consisted of a $LiNi_{0.6}Mn_{0.2}Co_{0.2}O_2$ cathode and a graphite anode. All battery studies were conducted using a battery cycler system (Neware BTS-4000; Neware Technology Co. Ltd. China). Electrochemical tests

were performed at various C-rate modes and 2.75 and 4.2 V for rapid cell deterioration. The detailed test conditions and evaluation environments are presented in Table 1 and Fig. 4, respectively. All C-rates were calculated based on the nominal capacity specified by the manufacturer. The test conditions are divided into two categories, referred to as Cases 1 and 2. Case 1 represents the condition for charging at 0.5 C, whereas Case 2 represents the condition of charging at 1 C. Except for the charging condition, all other conditions, such as the discharge and rest conditions, were the same.

4. Results and Discussion

The experimental results of Case 1 are shown in Fig. 1a, where each test period is divided into basic and accelerated operation periods. The main objective of this work is to find the effect of various battery utilization on battery degradation. Although battery utilization varies, we need common charge/discharge operations to compare each condition at the same baseline. With these basic operation experiments, the battery is settled in a normal state, and accelerated operation periods would be regarded as a source of degradation model in our manuscript. In the basic operation period, the 0.5 C charge condition and 0.2 C discharge condition were repeated three times. In the acceleration operation period, the charging process is the same at 0.5 C but the discharging process proceeds for one cycle at 0.5, 1.0, and 2.0 C. As the discharge current increased during the cycle, the degradation in the discharge capacity became relatively high.

Fig. 1b shows the experimental results for Case 2. The basic operation period of Case 2 is the same as that of Case 1, except for the acceleration operation period during the test period. In Case 2, the acceleration operation period is the same as in Case 1, except for charging at 1.0 C. Compared with the result of Case 1, the degradation of the basic operation period in Case 2 is very severe. It was confirmed that the battery capacity was significantly reduced when the charging current was high.

Fig. 2 shows a comparison of the charge/discharge capacity and coulombic efficiency of the 1st and 45th sets of Cases 1 and 2 under different test conditions. Detailed capacity values are shown in Table S1. Fig.

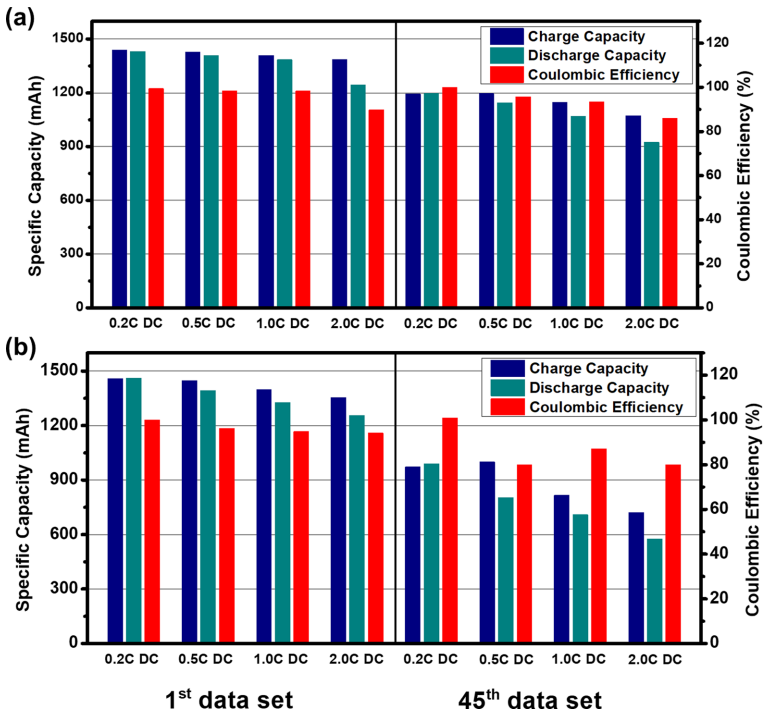

Fig. 2. Comparison of the charge/discharge capacity and coulombic efficiency of the 1st and 45th sets of Cases (a) 1 and (b) 2 under different test conditions.

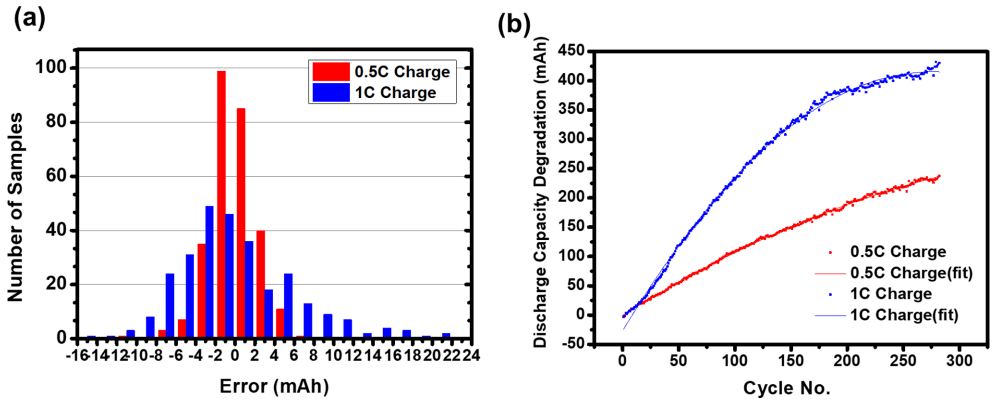

Fig. 3. The fitting (a) errors and (b) results of the discharge capacity degradation estimations from base operations for different charging capacity test cases.

2a,b represent the values of the 1st and 45th datasets in Cases 1 and 2, respectively. One dataset contains four discharge conditions. In Case 1, a capacity of 900 mAh or more is maintained under the discharge condition corresponding to 2.0 C DC in the 45th dataset, whereas in Case 2, the discharge capacity does not even reach 600 mAh. Overall, the results of Cases 1 and 2, which were similar in the initial 1st dataset, show a significant difference in the 45th dataset, which means 270 cycles.

Fig. 2a,b represent the values of the 1st and 45th datasets for Cases 1 and 2, respectively. Each dataset contained four discharge conditions. In Case 1, a capacity of 900 mAh or more is maintained under a discharge condition corresponding to 2.0 C DC in the 45th dataset. However, in Case 2, the capacity did not even reach 600 mAh. Overall, the results of Cases 1 and 2, which were similar in the initial 1st dataset, show a significant difference in the 45th dataset, which means 270 cycles. The results are summarized in Table S1. In Case 1, the discharge current in the 45th dataset was 1197 mAh, whereas in Case 2, it was reduced by approximately 17% to 989 mAh. The capacity fading is as follows: In Case 1, the capacity fading was 74% under the 0.5 C charge and 2.0 C discharge conditions. On the other hand, in Case 2, the capacity fading was 46% under the 1.0 C charge and 2.0 C discharge conditions. As the data shows, a mild charging condition of 0.5 C provides more stable data flow than a relatively high 1 C charging condition. In particular, data with a reversal of coulombic efficiency is observed at 1 C charging conditions compared to 0.5 C discharging conditions. This may reduce the accuracy of predictions of battery performance. Therefore, when determining the performance of reused batteries or batteries without usage information, serious consideration must be given to the C-rate during charging rather than discharging. This will actually contribute to maintaining more efficient battery performance as well as securing stable data that can increase the predictability of battery performance.

Fig. 3 shows the fitting results of Eq. (1) for the base operations of Cases 1 and 2. The accelerated C-rate results are eliminated and the interpolated values between the base operations for the adjacent test periods are displaced with the eliminated result values. As shown in Fig. 3a, the variation and error increased when the charging conditions were harsh. To fit the experimental data, as shown in Fig. 3b, α was set to 1. For Case 1, a was 1.204, a' was −0.001284, β was 2, b_0 was −0.8469, and the root mean square error (RMSE) was 39.44. For Case 2, a was 3.2, a' was −0.005784, β was 2, b_0 was −27.28, and RMSE was 100.4. Fig. 3a shows the error between the experimental discharge degradation and model-based discharge degradation values. In the two experimental cases, except for the charging conditions in Cases 1 and 2, the remaining electrochemical measurement conditions were the same. However, the degree of degradation of the discharge capacity was completely different. The deterioration linearity of Case 1 was broken in Case 2. In other words, the charging conditions significantly affect the cycling ability of the batteries.

Table 1. Test procedure for 18650 cells following a (a) 0.5 C charging condition for Case 1 and (b) 1.0 C charging condition for Case 2

(a) Case 1 (0.5 C)		(b) Case 2 (1.0 C)	
Step	Description	Step	Description
Basic Operation Period		Basic Operation Period	
1	Charge to 4.2 V @ 0.5 C	1	Charge to 4.2 V @ 0.5 C
2	Discharge to 2.75 V @ 0.2 C	2	Discharge to 2.75 V @ 0.2 C
3	Repeat steps 1–2 for 3 cycle	3	Repeat steps 1–2 for 3 cycle
Acceleration Operation Period		Acceleration Operation Period	
4	Charge to 4.2 V @ 0.5 C	4	Charge to 4.2 V @ 1.0 C
5	Discharge to 2.75 V @ 0.5 C	5	Discharge to 2.75 V @ 0.5 C
6	Repeat steps 4–5 for 1 cycle	6	Repeat steps 4–5 for 1 cycle
7	Charge to 4.2 V @ 0.5 C	7	Charge to 4.2 V @ 1.0 C
8	Discharge to 2.75 V @ 1.0 C	8	Discharge to 2.75 V @ 1.0 C
9	Repeat steps 7–8 for 1 cycle	9	Repeat steps 7–8 for 1 cycle
10	Charge to 4.2 V @ 0.5 C	10	Charge to 4.2 V @ 1.0 C
11	Discharge to 2.75 V @ 2.0 C	11	Discharge to 2.75 V @ 2.0 C
12	Repeat steps 10–11 for 1 cycle	12	Repeat steps 10–11 for 1 cycle
13	Repeat steps 1–12 for 45 times	13	Repeat steps 1–12 for 45 times

30-min rest following all charge and discharge steps

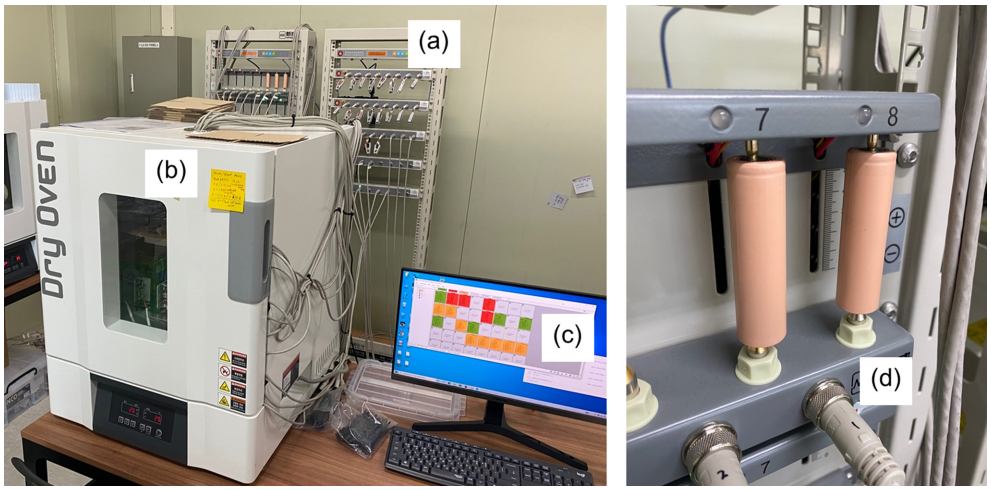

Fig. 4. Experimental setup: (a) battery cycler, (b) environment chamber, (c) battery cycler software, and (d) 18650 test cell.

5. Conclusions

Previous studies have mainly focused on the degradation model of certain parameters, such as the voltage and current. In practice, batteries experience variable charge/discharge conditions. In this study, it was determined that even when the base operation is mild and constant, the battery capacity is highly stimulated by the former charge and discharge conditions. It was not important to predict the number of battery

cycles under certain conditions since our goal was to predict the SOH and reusability of the battery. By employing empirical parameters and functions for the former charge and discharge conditions, we effectively observed the SOH of the battery. In future work, we need to generalize the formulation and parameters of the capacity degradation model with empirical parameters. This study only introduced an empirical model of battery experiences. Therefore, the specific values of the model should be derived with intensive experiments of various well-defined empirical conditions for battery usage.

Acknowledgements

This research was supported by the KIST Institutional Program (Project No. 2E33270) and the National Research Foundation of Korea (NRF-2022M3J1A1054151) funded by the Ministry of Science and ICT.

References

[1] Y. Li, K. Liu, A. M. Foley, A. Zülke, M. Berecibar, E. Nanini-Maury, J. V. Mierlo, and H. E. Hoster, *Renew. Sustain. Energy Rev.*, **2019**, *113*, 109254.
[2] S. Saxena, D. Roman, V. Robu, D. Flynn, and M. Pecht, *Energies*, **2021**, *14(3)*, 723.
[3] D. Šeruga, A. Gosar, C. A. Sweeney, J. Jaguemont, J. V. Mierlo, and M. Nagode, *Energy*, **2021**, *215*, 119079.
[4] S. Son, S. Jeong, E. Kwak, J. Kim, and K.-Y. Oh, *Energy*, **2022**, *238*, 121712.
[5] K.-J. Chung and C.-C. Hsiao, Accelerated degradation assessment of 18650 lithium-ion batteries, *2012 International Symposium on Computer, Consumer and Control*, Taichung, Taiwan, **2012**, 930–933.
[6] K. A. Severson, P. A. Attia, N. Jin, N. Perkins, B. Jiang, Z. Yang, M. H. Chen, M. Aykol, P. K. Herring, D. Fraggedakis, M. Z. Bazant, S. J. Harris, W. C. Chueh, and R. D. Braatz, *Nat. Energy*, **2019**, *4*, 383–391.
[7] M. A. Kamali, A. C. Caliwag, and W. Lim, *IEEE Embedded Systems Letters*, **2021**, *13(4)*, 206–209.
[8] S. Saxena, Y. Xing, D. Kwon, and M. Pecht, *Int. J. Electr. Power Energy Syst.*, **2019**, *107*, 438–445.
[9] A. Carnovale and X. Li, *Energy Ai*, **2020**, *2*, 100032.
[10] M. Varini, P. E. Campana, and G. Lindbergh, *J. Energy Storage*, **2019**, *25*, 100819.
[11] N. Yang, Y. Fu, H. Yue, J. Zheng, X. Zhang, C. Yang, and J. Wang, *Electrochim. Acta*, **2019**, *311*, 8–20.
[12] J. Park, W. A. Appiah, S. Byun, D. Jin, M.-H. Ryou, and Y. M. Lee, *J. Power Sources*, **2017**, *365*, 257–265.
[13] B. Xu, W. Diao, G. Wen, S.-Y. Choe, J. Kim, and M. Pecht, *J. Power Sources*, **2021**, *510*, 230390.
[14] C. Zhang, I. Chuckpaiwong, S. Y. Lian, and B. B. Seth, *Mech. Syst. Signal Process.*, **2002**, *16(4)*, 705–718.